Negative plasmon dispersion in $2H$-NbS$_2$ beyond charge-density-wave interpretation

Pierluigi Cudazzo[1,2], **Eric Müller**[3], **Carsten Habenicht**[3], **Matteo Gatti**[1,2,4], **Helmuth Berger**[5], **Martin Knupfer**[3], **Angel Rubio**[6,7], **Simo Huotari**[8]

1 Laboratoire des Solides Irradiés, École Polytechnique, CNRS, CEA, Université Paris-Saclay, F-91128 Palaiseau, France

2 European Theoretical Spectroscopy Facility (ETSF)

3 IFW Dresden, P.O.Box 270116, D-01171 Dresden, Germany

4 Synchrotron SOLEIL, L'Orme des Merisiers, Saint-Aubin, BP 48, F-91192 Gif-sur-Yvette, France

5 École Polytechnique Fédérale de Lausanne (EPFL), Institut de Physique des Nanostructures, CH-1015 Lausanne, Switzerland

6 Max Planck Institute for the Structure and Dynamics of Matter, Luruper Chaussee 149, 22761 Hamburg, Germany

7 Nano-Bio Spectroscopy Group and European Theoretical Spectroscopy Facility (ETSF), Universidad del País Vasco CFM CSIC-UPV/EHU-MPC DIPC, 20018 San Sebastián, Spain

8 Department of Physics, P.O.Box 64, FI-00014 University of Helsinki, Finland

E-mail: `angel.rubio@ehu.es`

Abstract. We examine the experimental and theoretical electron-energy loss spectra in $2H$-Cu$_{0.2}$NbS$_2$ and find that the 1 eV plasmon in this material does not exhibit the regular positive quadratic plasmon dispersion that would be expected for a normal broad-parabolic-band system. Instead we find a nearly non-dispersing plasmon in the momentum-transfer range $q < 0.35$ Å^{-1}. We argue that for a stoichiometric pure $2H$-NbS$_2$ the dispersion relation is expected to have a negative slope as is the case for other transition-metal dichalcogenides. The presence of Cu impurities, required to stabilize the crystal growth, tends to shift the negative plasmon dispersion into a positive one, but the doping level in the current system is small enough to result in a nearly-non-dispersing plasmon. We conclude that a negative-slope plasmon dispersion is not connected with the existence of a charge-density-wave order in transition metal dichalcogenides.

PACS numbers: 71.45.Lr, 71.45.Gm, 79.20.Uv, 73.21.Ac

1. Introduction

The charge density wave (CDW) is a broken symmetry state of metals induced by electron-phonon or by electron-electron interactions. The ground state is the coherent superposition of electron-hole pairs, and, as the name implies, the corresponding charge density is not uniform but displays a periodic spatial variation. Usually, the CDW phase transition is accompanied by the appearance of an energy gap or pseudo gap in the electronic band structure, phonon softening and lattice distortions. Layered transition-metal dichalcogenides (TMD)[1] are prototypical materials displaying CDW instability and for this reason they have attracted considerable interest in the last years[2]. However, although extensively studied, a clear understanding of the physical mechanism responsible for the appearance of CDW order in this class of materials is still missing[3]. In particular, several explanations have been put forward: from Fermi surface nestings[4] to van Hove singularities (saddle points) in the density of states (DOS)[5], until a recent theoretical work that pointed to the role of electron-phonon coupling, ruling out a pure electronic mechanism for the CDW instability[6].

In general, since a generic electronic instability induces a strong enhancement of the charge-charge response function, this quantity plays a crucial role in detecting CDW order not only from a theoretical point of view but also experimentally. As a matter of fact, being related to the inverse macroscopic dielectric function, it can be directly measured in electron energy loss spectroscopy (EELS) and in inelastic X-ray scattering (IXS) experiments.

In this context, J. van Wezel and coworkers[7] have established a direct link between CDW instability and collective excitations (plasmons) that represent the poles of the charge-charge response function. EELS measurements in three prototypical TMDs belonging to the $2H$ family ($2H$-TaS$_2$, $2H$-TaSe$_2$ and $2H$-NbSe$_2$)[7, 8, 9] revealed a dispersion relation that had a negative slope, i.e., the plasmon energy was found to decrease with an increasing momentum transfer. In this case the dispersion is said to be negative. This is in contrast with the case of a homogeneous electron gas (the jellium model), where the plasmon has a positive parabolic dispersion. On the basis of a macroscopic semiclassical Ginzburg-Landau model, it was suggested that the negative dispersion in TMD is the consequence of the collective charge fluctuations associated with the CDW order identifying a direct connection between CDW instability and plasmon dispersion.[7] This picture was supported by the fact that for $2H$-NbS$_2$, the only system belonging to the $2H$ family that does not display CDW order, the available experimental results pointed out that the plasmon dispersion had a positive slope[10].

Nevertheless, a negative plasmon dispersion has been found also in several other materials that do not display CDW instability, for example doped molecular crystals[11]. Even alkali metals[13, 14, 15, 16, 17, 18, 19, 20] have been shown to exhibit several deviations from the jellium model including negative plasmon dispersion. Starting from this observation, a different interpretation of the negative plasmon dispersion in $2H$-TMDs has been given on the basis of first principle calculations [21, 22, 23]. As shown

in Ref. [22], the unusual dispersion in this class of materials is due to the peculiar behavior of intraband transitions that contribute to the plasmon excitation. If the negative plasmon dispersion is a pure band effect, a similar behaviour should also be present in NbS$_2$ contrary to the experimental observation[10]. However, it is important to note that stoichiometric pure NbS$_2$ is difficult to grow since 2H-NbS2 is unstable in the growth process[8] unless metallic impurities are present. A possible positive dispersion could be an effect of impurities that are required to stabilize the system. Such an effect of metal impurities on the intraband plasmons in TMDs was shown by utilizing the rigid-band model and time-dependent density functional theory (TDDFT) [22]. Good agreement between TDDFT calculations and IXS spectra at high energy and large momentum transfer was indeed recently found for NbSe$_2$ and Cu$_{0.2}$NbS$_2$ [24].

Motivated by these observations, we combined EELS experiments and first-principle TDDFT calculations, and investigated the collective excitations and their dispersion as a function of the momentum transfer in 2H-Cu$_{0.2}$NbS$_2$ with the aim to clarify the origin of the negative plasmon dispersion in TMDs. From our measurements we did not find a positive quadratic dispersion in this system, in contradiction to what has been reported before. Earlier TDDFT-based work [22] predicted that the dispersion would be in fact negative if the concentration of Cu would be small enough. Based on our new experimental findings, that match well the prediction of TDDFT, we argue that the negative plasmon dispersion is a general property of 2H-TMDs related to the particular band structure of these materials and that there is no need to invoke a coupling with the CDW.

2. Methods

2.1. Experiment

The Cu$_{0.2}$NbS$_2$ crystal was grown by vapor transport using iodine as a transport agent.[12] The stoichiometry was verified by standardless energy dispersive spectrometry using a Jeol JXA-8600 electron probe microanalyzer. The EELS measurements along ΓM crystallographic direction ($\mathbf{q} \parallel [100]$) were performed with a 172-keV spectrometer described in Refs. [30, 31]. The momentum resolution was set to 0.04 Å^{-1} and the energy resolution to 85 meV. The sample temperature was controlled using a He flow cryostat, and measurements were done at $T = 20$ K and at room temperature. No particular difference between the results at different temperatures was found, except for a blueshift of the plasmon energy by ∼0.04 eV upon cooling to 20 K. In the following, we concentrate on the data taken at 20 K. The electron beam spot size on the sample was ∼0.5 mm. The quasielastic zero-loss peak line's tail was subtracted from the measured spectra by fitting a suitable Pearson VII function to the data for energy transfer (ω) between 0.1 and 0.3 eV.

The crystal used in the experiment was found to have a well defined stoichiometry of Cu$_x$NbS$_2$, with energy-dispersive x-ray spectroscopy revealing $x =$0.17–0.18 with the Cu

atoms sitting in the interstitial region between the NbS$_2$ layers (hence for the remaining of the article we indicate here the value $x \approx 0.2$). The high quality of the crystal was verified by measuring the electron diffraction pattern.

2.2. Computational details

The microscopic complex dielectric function $\epsilon = \epsilon_1 + i\epsilon_2$ is related to the susceptibility χ (Ref. [25]) by the relation: $\epsilon^{-1} = 1 + v\chi$ (v being the Coulomb potential). In TDDFT χ is the solution of the Dyson like equation: $\chi = \chi_0 + \chi_0(v + f_{xc})\chi$, where χ_0 is the Kohn-Sham (KS) susceptibility expressed in terms of KS eigenenergies and eigenfunctions, while f_{xc} is the exchange-correlation kernel, for which we use the random phase approximation (RPA) ($f_{xc} = 0$)‡. The Fourier components of both χ and ϵ are matrices in terms of the reciprocal lattice vectors $\mathbf{G}$. The macroscopic dielectric function ϵ_M is given by $\epsilon_M(\mathbf{q}, \omega) = 1/\epsilon_{\mathbf{GG}}^{-1}(\mathbf{q}, \omega)$, where $\mathbf{q}$ is inside the first Brillouin zone. The loss function $L(\mathbf{q}, \omega)$ measured in EELS experiments is directly related to the imaginary part of the inverse macroscopic dielectric function through the following equation: $L(\mathbf{q}, \omega) = -\mathrm{Im}\,\epsilon_M^{-1}(\mathbf{q}, \omega)$.

In the present work the KS eigenenergies and eigenfunctions used to determine χ_0 have been evaluated in the local-density approximation (LDA) implemented in a plane-wave-based code[26]. In our calculations we adopt the experimental lattice parameters[27]. We use Troullier-Martins and Hartwigsen-Goedecker-Hutter norm-conserving pseudopotentials [28] (with an energy cutoff of 120 Ry). In the calculation of χ_0 (Ref. [29]), we used a $24 \times 24 \times 12$ grid of $\mathbf{k}$ points and included 100 bands. The macroscopic dielectric function has been obtained inverting a matrix of 300 $\mathbf{G}$ vectors (those parameters lead to converged results for the response function in the range of energies and momentum studied in the present work). Finally, the electron doping induced in NbS$_2$ by the Cu atoms has been simulated by shifting the Fermi level upward according to the rigid-band model (in the present case this is equivalent to add 0.4 electrons per unit cell). An intrisic lifetime broadening of 0.05 eV was used in the calculation of the complex dielectric functions, and the loss functions obtained from the them were additionally convoluted with a Gaussian with a full width at half maximum of 0.085 eV to match the experimental energy resolution.

3. Results and discussion

The computed and measured loss function in $2H$-Cu$_{0.2}$NbS$_2$ are shown in Fig. 1 for various momentum transfers along the ΓM direction. In both cases, the loss spectrum is characterized by a peak that resides at ~ 1 eV. This structure is related to the collective excitations of the d_z states of the Nb atoms[11]. It should be noted that the plasmon frequency obtained from the electronic density corresponding to these states

‡ We note that exchange-correlation effects beyond RPA in this class of materials are not changing qualitatively the results[22, 24].
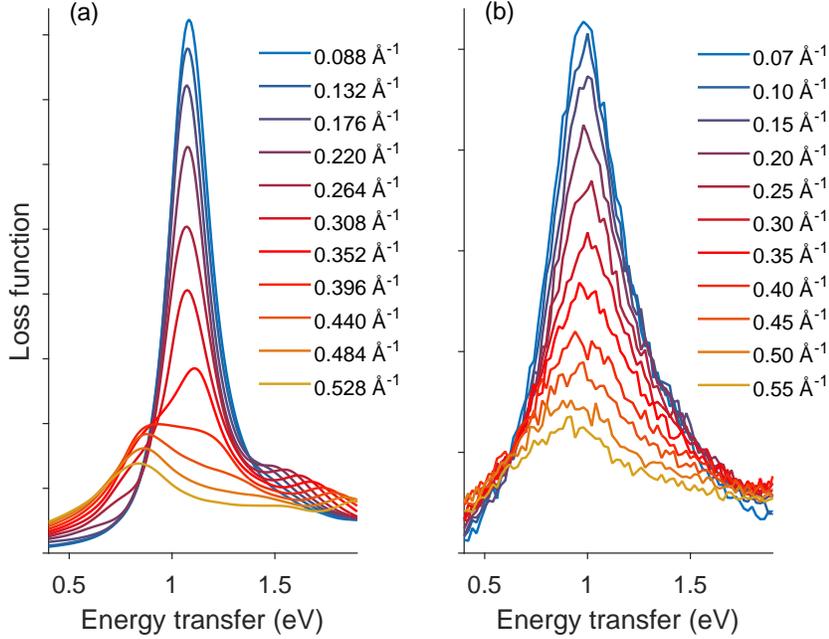
Figure 1. (Color online) Loss functions for $2H\text{-}Cu_{0.2}NbS_2$ based on (a) TDDFT calculation and (b) EELS experiment for several momentum transfers indicated in the legends.

(2.4 electrons per unit cell) overestimates the observed frequency by about 4 eV. This overestimation is related to the presence of interband transitions that screen the bare plasmon frequency and are absent in the jellium model. The peak is decreasing in intensity and broadening when the momentum transfer is increased. The dispersion of its energy as a function of momentum transfer is nearly negligible when $q < 0.35$ Å^{-1}. The results of the experiment and theory are in excellent agreement. Interestingly, the dispersion seems to show a somewhat anomalous behavior for $q > 0.35$ Å^{-1}. From the experimental spectra one might conclude that the plasmon energy starts to shift to smaller values with increasing q above $q > 0.35$ Å^{-1}. The reason for this becomes apparent when the theoretical spectra are carefully examined. At $q = 0.352$ Å^{-1}, the theoretical loss function peak position increases rapidly with an increasing q, with a lower-energy peak appearing at ~ 0.8–0.9 eV. This lower-energy peak steals most of the spectral weight at the highest studied q. The experimental spectra show the same overall behavior, while due to the generally broader features the two structures are not individually resolved. However, comparison with the theoretical spectra reveals uniquely the reason for the seemingly negative plasmon behavior in this momentum-transfer range.

To gain further insight into the behaviour of the plasmon in this range of momentum transfer, we compare in Fig. 2 the loss function with the real (ϵ_1) and imaginary (ϵ_2) parts of the dielectric function evaluated between 0.22 and 0.4 Å^{-1}. As we can see, for a small q, the 1-eV plasmon is caused by ϵ_1 crossing zero. This behavior has been
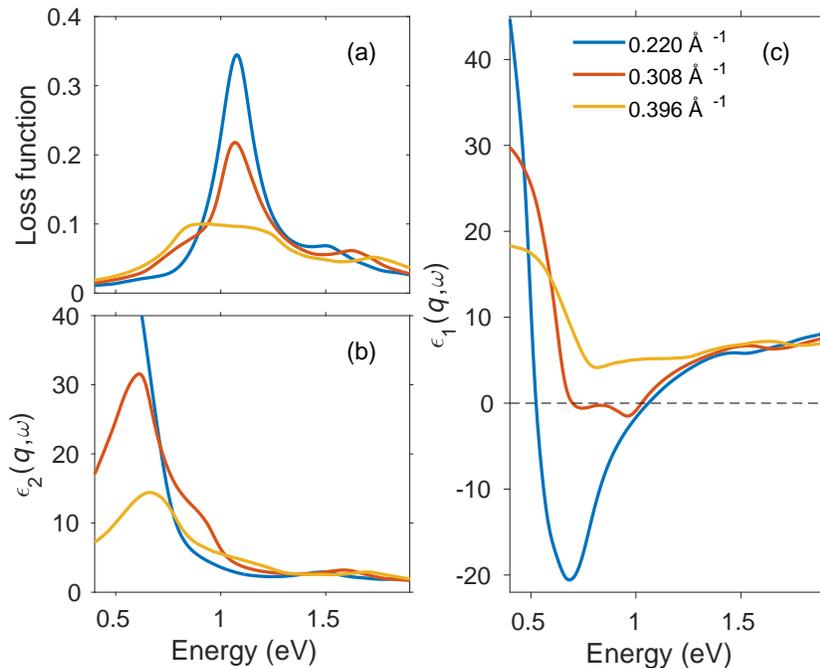
Figure 2. (Color online) (a) The loss function, (b) the imaginary and (c) real part of the dielectric function for Cu$_{0.2}$NbS$_2$ for three selected momentum transfers.

shown previously to correspond to intraband transitions involving bands that cross the Fermi energy[11]. However, at $q = 0.31$ Å^{-1} a shoulder appears in ϵ_2 just above the main intraband peak. Because ϵ_1 and ϵ_2 are related through the causality relation, this shoulder causes an oscillation in the real part of the dielectric function. This, in turn, increases the number of zero crossings of the real part. This explains the appearance of a double structure in the loss function as seen in Fig. 1. Thus, beyond $q = 0.35$–0.4 Å^{-1} it is not possible to clearly identify the position of the plasmon frequency since in this range of momentum transfer the loss function obtains a relatively complex multiple-peak structure. At larger q the oscillation in ϵ_1 disappears. However, for $q > 0.40$ Å^{-1} the real part of the dielectric function does no longer cross zero. This means the plasmon is no longer well defined since it decays into electron-hole excitations, and the e-h continuum is probed. It is noteworthy that even at smaller momentum transfers the plasmon is strongly damped.

The extraction of the dispersion from the plasmon is, based on the discussion above, a convoluted problem owing to the peculiar behavior of the dielectric function and the appearance of the doublet feature. We nevertheless present here the *apparent* energy of the loss-function peak as a function of q, of both experimental and theoretical spectra. The peak position has been determined by fitting a Gaussian peak near the top of the plasmon peak in both cases. The uncertainty of the experimental peak positions has been determined by simulating how much the resulting peak position varies when additional random noise within the statistical errorbar is added to the
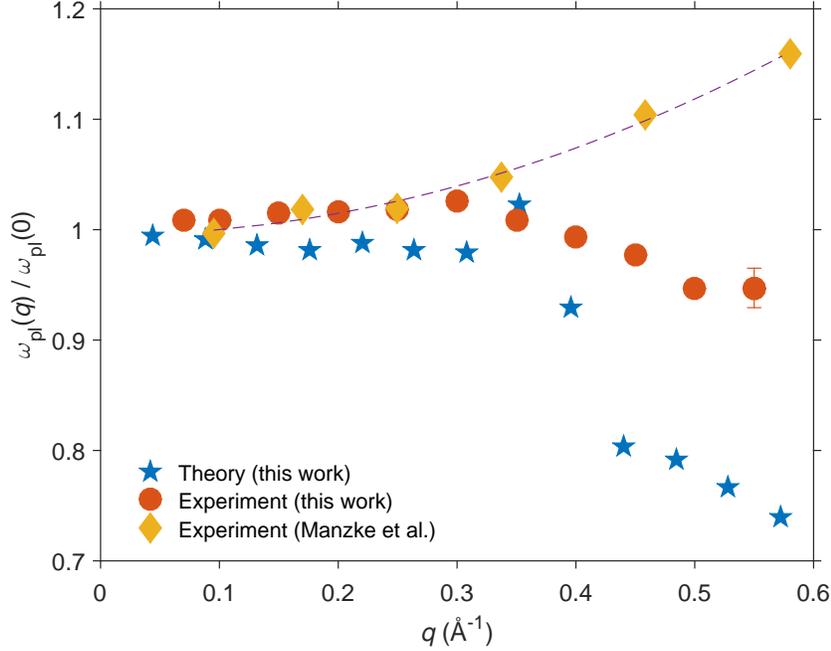
Figure 3. (Color online) Plasmon dispersion for $Cu_{0.2}NbS_2$ as a function of q for experiment, theory, and compared to published results for NbS_2 (Ref. [10]). The dashed line is a quadratic fit to the data points of Ref. [10].

data, performing the fit multiple times in this way, and taking the statistical 1σ of the result as the uncertainty of the fit. This dispersion is shown in Fig. 3, for plasmon energies renormalized to values extrapolated to $q = 0$, i.e., $\omega_{pl}(q)/\omega_{pl}(0)$, which from the various sources is $\omega_{pl}(0) \approx 0.95$ eV (Ref. [10]), ≈ 0.98 eV (current experiment), and ≈ 1.09 eV (current theory). From Fig. 3 it can be seen that while the published results from Ref. [10] show a positive, close to quadratic, upward slope of the plasmon energy versus q as expected for a plasmon in homogeneous electron gas, our experiment and theory show much weaker dispersion until $q = 0.3$ Å^{-1}, after which the dispersion becomes negative, owing to the reasons explained above.

It was theoretically shown by some of us [22] that $2H$-TMDs in general are expected to exhibit negative plasmon dispersions for pure stoichiometric systems, but metallic dopants are expected to affect the dispersion curve, switching it to a positive dispersing one. This is in agreement with experimental results on several doped TMD compounds (Refs. [8, 32, 33]). In our case, therefore, it can be deduced that in $Cu_{0.2}NbS_2$ the level of Cu-doping is enough to flatten the dispersion curve, but not high enough to switch it into a monotonically increasing one.

The difference between our new results and than those obtained in Ref. [10] should be attributed to the presence of impurities in the samples of both studies. However, in our case it can be argued that the low density of Cu impurities is not enough to fully switch the plasmon dispersion into a quadratic one. This result is expected based on the prediction of modeling the doping by a rigid-band shift as was done in Ref. [22].

4. Conclusions

We have shown that in $2H$-$Cu_{0.2}NbS_2$ the plasmon dispersion curve is relatively flat instead of a positive dispersion observed in a previous study. We have compared the experimental loss function of $2H$-$Cu_{0.2}NbS_2$ to one calculated within the TDDFT, which we in turn analyze in detail by breaking it up into the real and imaginary part of the dielectric function. Together with comparison to earlier literature on other TMDs of the $2H$ family we conclude that our results corroborate the picture proposed by some of us in Ref.[22]: the measured negative plasmon dispersion is a basic property of all TMDs belonging to the $2H$ family and is directly related to the shape of the bands crossing the Fermi level that is similar in this class of materials. Moreover, as it has been shown in previous theoretical and experimental works[22, 8, 32, 33], electron doping beyond a given threshold, which depends on the system, switches the plasmon dispersion to have a positive slope. This means that an inclusion of metallic dopants, required to stabilize NbS_2 upon growth, will affect the dispersion curve, having a tendency to switch it to a monotonically increasing one. In conclusion, these results support the interpretation that the negative plasmon dispersion is a property of all undoped 2H compounds, independently of having a CDW order or not. Therefore it should not be attributed directly to a possible interplay of the electronic excitations and CDW ordering.

[1] J. A. Wilson and A. D. Yoffe. Adv. Phys. **18**, 193 (1969).
[2] T. Kiss, *et al.*, Nat. Phys. **3**, 720 (2007); S. V. Borisenko, *et al.*, Phys. Rev. Lett. **100**, 196402 (2008); S. V. Borisenko, *et al.*, *ibid.* **102**, 166402 (2009).
[3] For a recent review, see e.g. K. Rossnagel, J. Phys. Condens. Matter **23**, 213001 (2011).
[4] J. A. Wilson, F. J. Di Salvo, and S. Mahajan, Phys. Rev. Lett. **32**, 882 (1974).
[5] T. M. Rice and G. K. Scott, Phys. Rev. Lett. **35**, 120 (1975).
[6] M. D. Johannes, I. I. Mazin, and C. A. Howells, Phys. Rev. B **73**, 205102 (2006); M. D. Johannes and I. I. Mazin, *ibid.* **77**, 165135 (2008).
[7] J. van Wezel, *et al.*, Phys. Rev. Lett. **107**, 176404 (2011).

[8] R. Schuster, Ph.D. thesis, Technische Universität Dresden (Germany), 2009, http://nbn-resolving.de/urn:nbn:de:bsz:14-qucosa-27333

[9] R. Schuster, *et al.*, Phys. Rev. B **79**, 045134 (2009).

[10] R. Manzke, *et al.*, Solid State Commun. **40**, 103 (1981).

[11] P. Cudazzo, *et al.*, Phys. Rev. B **84**, 155118 (2011).

[12] F. Lévy and H. Berger, J. Cryst. Growth 61, 61 (1983)

[13] A. vom Felde, J. Sprösser-Prou, and J. Fink, Phys. Rev. B **40**, 10181 (1989).

[14] F. Aryasetiawan and K. Karlsson, Phys. Rev. Lett. **73**, 1679 (1994).

[15] A. Fleszar, R. Stumpf, and A. G. Eguiluz, Phys. Rev. B **55**, 2068 (1997).

[16] S. Huotari, *et al.*, Phys. Rev. B **80**, 155107 (2009).

[17] S. Huotari, *et al.*, Phys. Rev. B **84**, 075108 (2011).

[18] M. Cazzaniga, *et al.*, Phys. Rev. B **84**, 075109 (2011).

[19] I. Loa, K. Syassen, G. Monaco, G. Vankó, M. Krisch and M. Hanfland, Phys. Rev. Lett. **107**, 086402 (2011).

[20] H.-K. Mao, *et al.*, Proc. Nat. Acad. Sci. USA **108**, 20434 (2011).

[21] M. N. Faraggi, A. Arnau, and V. M. Silkin Phys. Rev. B **86**, 035115 (2012).

[22] P. Cudazzo, M. Gatti, and A. Rubio, Phys. Rev. B **86**, 075121 (2012).

[23] P. Cudazzo, M. Gatti, and A. Rubio, Phys. Rev. B **90**, 205128 (2014).

[24] P. Cudazzo, K. O. Ruotsalainen, Ch. J. Sahle, A. Al-Zein, H. Berger, E. Navarro-Moratalla, S. Huotari, M. Gatti, and A. Rubio, Phys. Rev. B **90**, 125125 (2014)

[25] G. Onida, L. Reining, and A. Rubio, Rev. Mod. Phys. **74**, 601 (2002).

[26] X. Gonze, G.-M. Rignanese, M. Verstraete, J.-M. Beuken, Y. Pouillon, R. Caracas, F. Jollet, M. Torrent, G. Zerah,M.Mikami, Ph. Ghosez, M. Veithen, J.-Y. Raty, V. Olevano, F. Bruneval, L. Reining, R. Godby, G. Onida, D. R. Hamann, and D. C. Allan, Z. Kristallogr. **220**, 558 (2005).

[27] E. Moncton, J. D. Axe, and F. J. Di Salvo, Phys. Rev. B **16**, 801 (1977); W. G. Fisher and M. J. Sienko, Inorg. Chem. **19**, 39 (1980); A. Meetsma, G. A. Wiegers, R. J. Haange, and J. L. de Boer, Acta Crystallogr. Sect. C **46**, 1598 (1990).

[28] N. Troullier and J. L. Martins Phys. Rev. B **43**, 1993 (1991); C. Hartwigsen, S. Goedecker, and J. Hutter, Phys. Rev. B **58**, 3641 (1998).

[29] A. Marini, C. Hogan, M. Gruning, and D. Varsano, Comput. Phys. Commun. **180**, 1392 (2009).

[30] F. Roth, A. König, J. Fink, B. Büchner, and M. Knupfer, J. El. Spectr. Rel. Phenom. 195, 85 (2014).

[31] J. Fink, Adv. El. El. Phys. 75, 121 (1989).

[32] A. König, K. Koepernik, R. Schuster, R. Kraus, M. Knupfer, B. Büchner, and H. Berger, EPL (Europhysics Letters) 100, 27002 (2012).

[33] E. Müller, B. Buchner, C. Habenicht, A. König, M. Knupfer, H. Berger, and S. Huotari, (submitted).